Reversible formation of tetraphenylpentalene, a room temperature stable antiaromatic hydrocarbon

Hugh J. Sanderson,[a] Andreas Helbig,[b] Gabriele Kociok-Köhn,[c] Holger Helten,*[b] Ulrich Hintermair*[a]

a)   Department of Chemistry and Institute for Sustainability, University of Bath, Claverton Down, Bath BA2 7AY, UK.
b)   Julius-Maximilians-Universität Würzburg, Institute of Inorganic Chemistry and Institute for Sustainable Chemistry & Catalysis with Boron, Am Hubland, 97074 Würzburg, Germany
c)   Physical Structure Characterisation, University of Bath, Claverton Down, Bath BA2 7AY, UK.

*holger.helten@uni-wuerzburg.de
*u.hintermair@bath.ac.uk

Supporting Information

Contents

Experimental

General Considerations: All reactions were conducted under argon using standard Schlenk techniques or a MBraun Unilab Plus glovebox, unless stated otherwise. All commercially available materials were purchased from Sigma Aldrich, Fisher or Acros.

Solvents: Methanol was dried and distilled over magnesium. Toluene was dried and distilled over sodium. THF, hexane and pentane were dried and distilled over potassium. C_6D_6 was distilled from CaH_2 and stored over 4Å molecular sieves.

Reagents: 1,3,4,6-tetraphenyl-1,2-dihydropentalene[1] and magnesium 1,3,4,6-tetraphenylpentalenide[2] were prepared according to literature procedures.

Analysis: NMR spectra were obtained using either a 500 MHz Bruker Avance III or a 400 MHz Bruker AvanceNeo spectrometer. Chemical shifts (δ) are given in ppm and referenced to residual proton chemical shifts from the NMR solvent for ^1H and $^{13}C\{^1H\}$ spectra. IR spectra were recorded on a Bruker Alpha II FT-IR spectrometer using a diamond ATR module. UV-vis spectroscopy was performed inside a MBraun Unilab Plus glovebox using an Avantes AvaLight-DH-S-BAL light source and an AvaSpec-2048L photospectrometer. Data was collected between 250 nm and 1000 nm with an integration time of 4 ms.

Single crystal X-ray diffraction analysis was carried out using a RIGAKU SuperNova, Dual,Cu a zero EoS2 single crystal diffractometer. Mass spectrometry was carried out at the Chemical Characterisation Facility at the University of Bath using a Bruker MaXis HD ESI-QTOF.

Computational methods: Optimization, NICS Scan[3], NICS XY-Scan,[4] ACID,[5,6] and TD-DFT calculations were carried out using the Gaussian 09 program package, revision D.01.[7] Becke's three parameter exchange-correlation hybrid functional B3LYP[8–12] was used in combination with the 6-311++G(d,p) basis set. The stationary points were characterized as minima by an analytical vibrational frequency calculation[13,14] which revealed the absence of imaginary frequencies. The NICS Z scan was performed perpendicular to the respective ring, from its center up to 4 Å above the plane, and the NICS Y scan at 1.7 Å above the respective subunits. The ACID calculation was plotted with an isovalue of 0.03. The optimised structure as well as the calculation setup for the NICS Z and the NICS Y scan are attached as .mol-files.

Synthesis of 1,3,4,6-tetraphenylpentalene

A freshly prepared THF solution of iodine (0.1 M, 1.5 mL, 0.15 mmol) was added to a THF solution of **Mg[Ph$_4$Pn]** (98 mg, 0.15 mmol) at room temperature. An immediate colour change from orange to dark red was observed followed by precipitation of a yellow solid. The reaction was allowed to stir for one hour before it was filtered, and the solution evaporated to dryness and kept under vacuum overnight to yield **1,3,4,6-Ph$_4$Pn** as a dark red powder (46 mg, 75%)
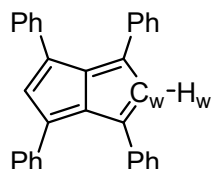
^{1}H NMR (500 MHz, THF-h$_8$) δ: 7.15-7.13 (m, 12H, ArH), 7.07-7.04 (m, 8H, ArH), 5.44 (s, 2H, H$_w$)

^{13}C{^{1}H} NMR (126 MHz, THF-h$_8$) δ: 147.9, 145.6, 135.1, 134.9 (C$_w$), 129.2, 128.5, 127.6

HRMS (APCI) *m/z*: [M+H]$^+$ Calculated for C$_{32}$H$_{23}$: 407.1794, Found: 407.1767

UV-vis (THF) λ: 312 nm (ε = 95,000 M^{-1}cm^{-1}), 460 nm (ε = 40,000 M^{-1}cm^{-1})

UV-vis (C$_6$D$_6$) λ: 275 nm (ε = 90,000 M^{-1}cm^{-1}), 460 nm (ε = 20,000 M^{-1}cm^{-1})

Spectroscopic Data

1,3,4,6-tetraphenylpentalene
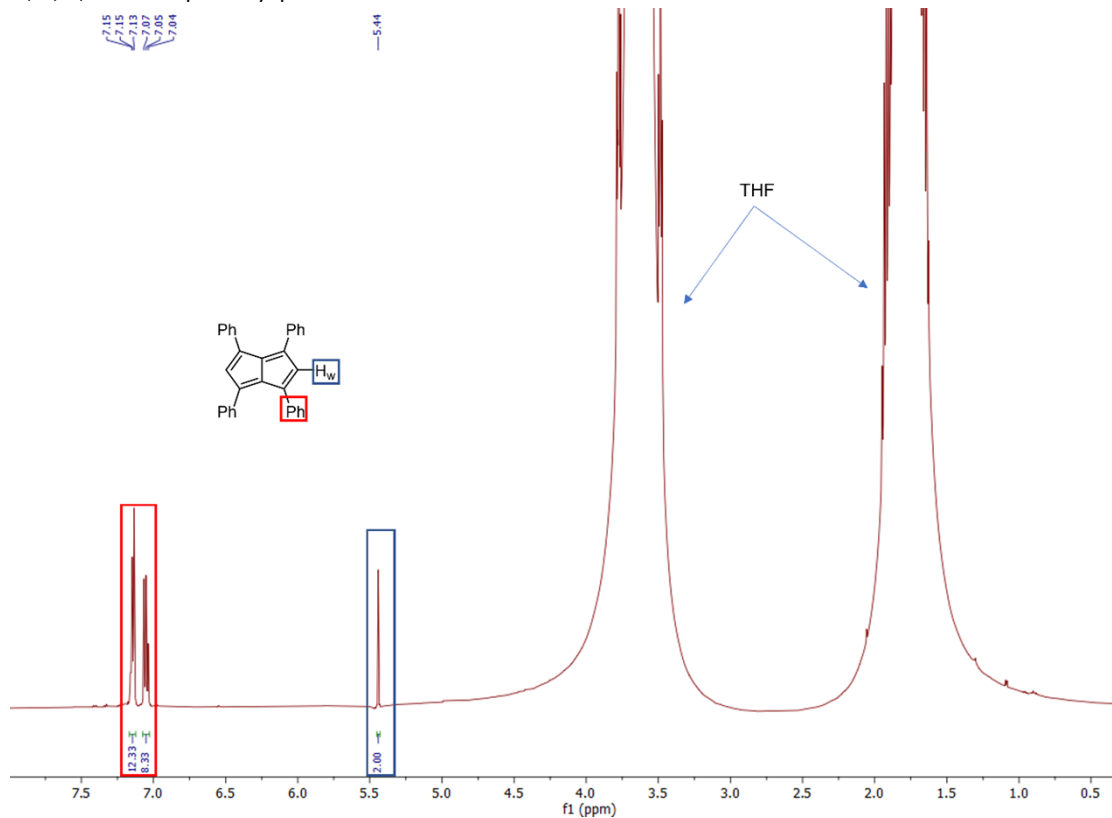
Figure S1: 500 MHz ^{1}H NMR spectrum of 1,3,4,6-tetraphenylpentalene in THF-H$_8$ recorded at room temperature.
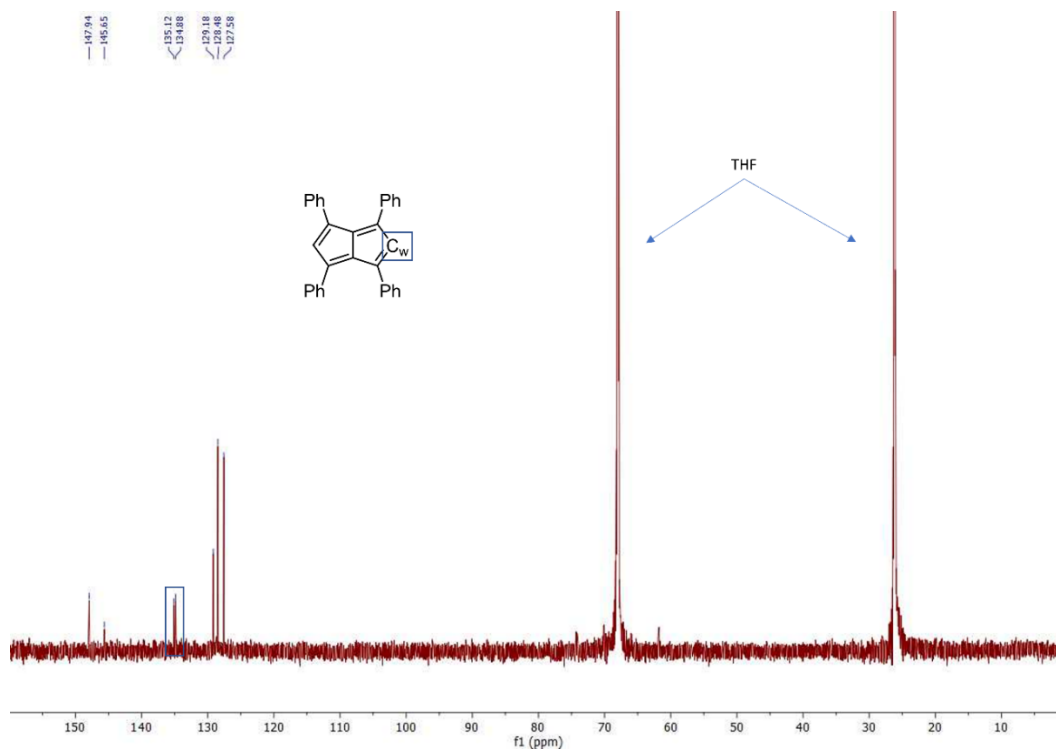
Figure S2: 125 MHz ^{13}C{^{1}H} NMR spectrum of **Ph$_4$Pn** in THF-H$_8$ recorded at room temperature.
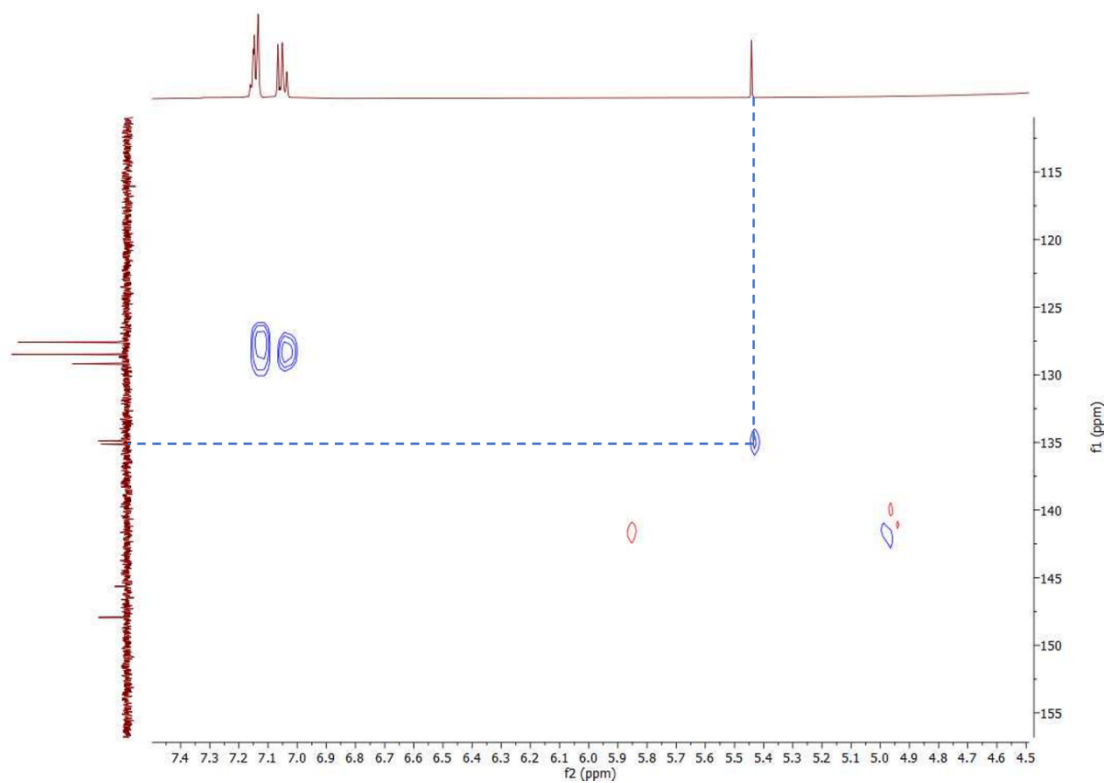
Figure S3: 500 MHz ^{1}H-^{13}C HSQC spectrum of 1,3,4,6-tetraphenylpentalene in THF-H$_8$ (H$_w$ = blue)
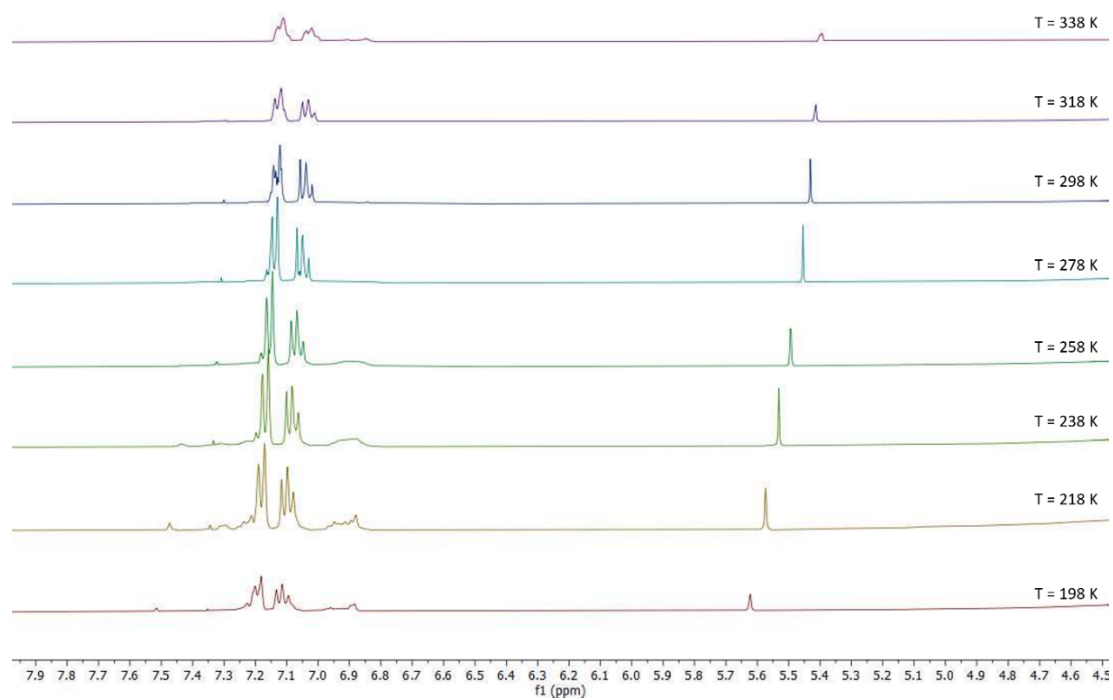
Figure S4: 400 MHz ^{1}H variable temperature NMR spectra of 1,3,4,6-tetraphenylpentalene in THF-H$_8$

Reduction with Potassium
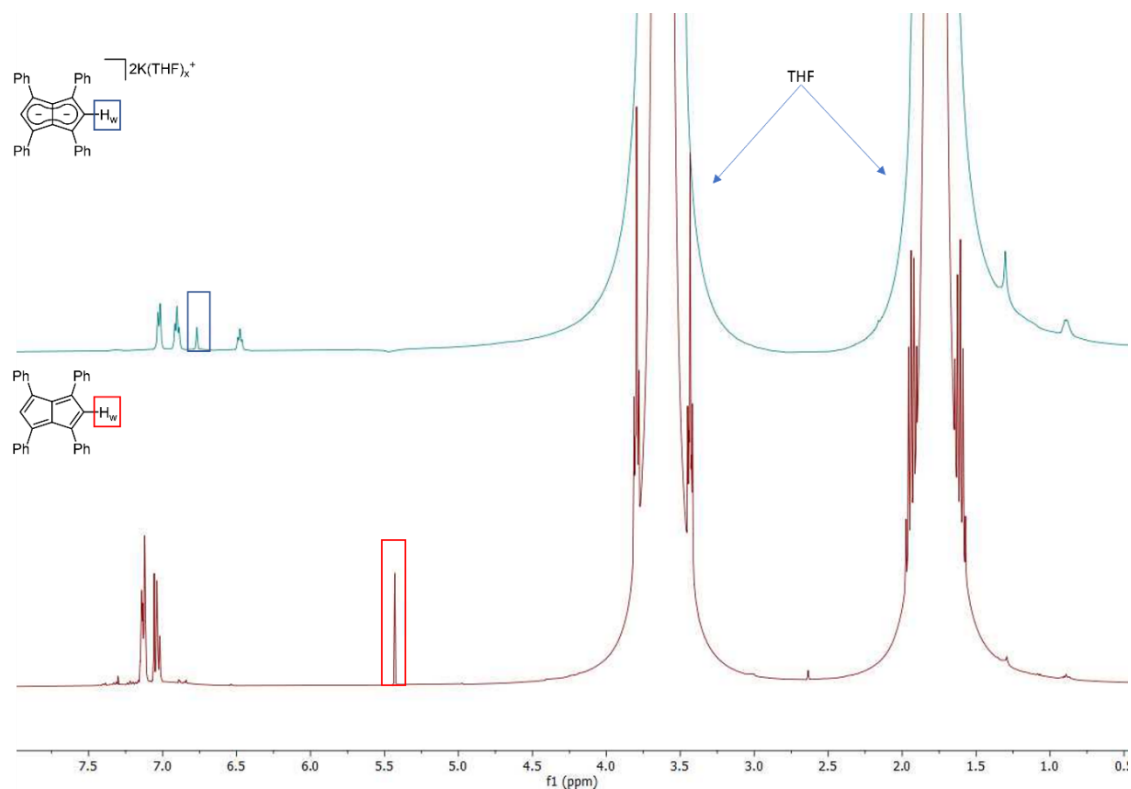
Figure S5: 500 MHz ^{1}H NMR spectra of **K$_2$[Ph$_4$Pn]** (top) formed by reaction of **Ph$_4$Pn** (bottom) with potassium in THF at room temperature.

Computational
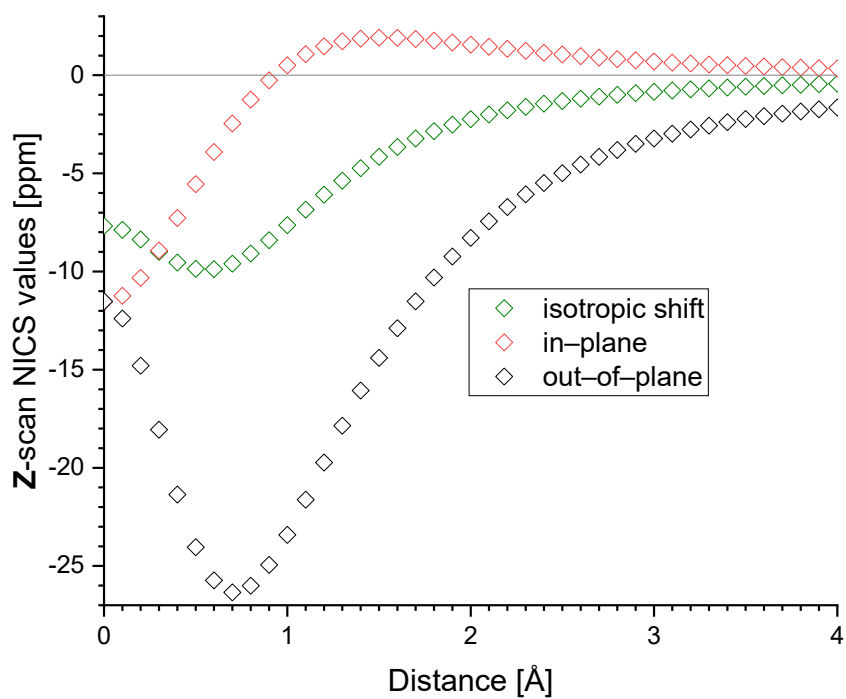
Figure S6: NICS Z scan through the centre of one of the flanking phenyl rings of **Ph₄Pn** using DFT calculations at the B3LYP/6-311++g(d,p) level of theory.
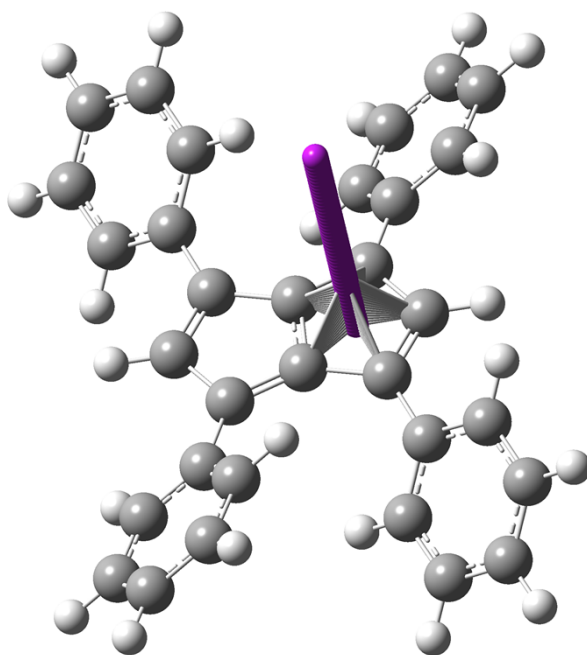
Figure S7: Placement of the Bq atoms for the NICS Z scan of the pentalene core of **Ph₄Pn**.
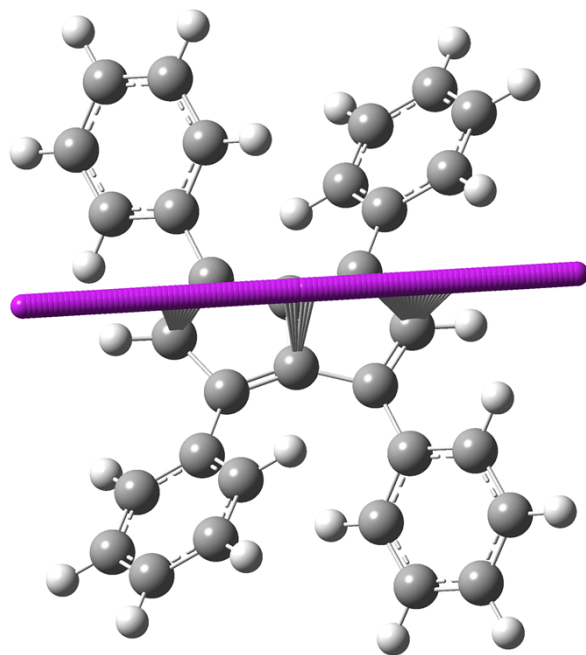
Figure S8: Placement of the Bq atoms for the NICS Y scan of the pentalene core of **Ph₄Pn**.
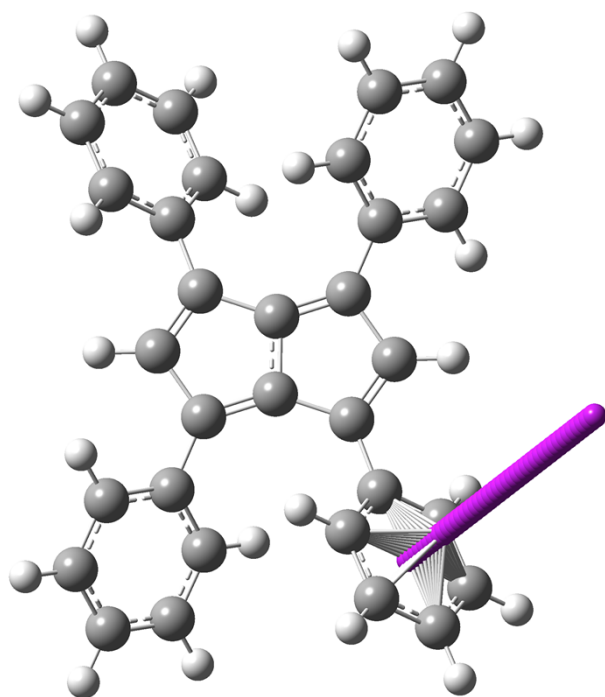
Figure S9: Placement of the Bq atoms for the NICS Z scan of one phenyl moiety of **Ph₄Pn**.
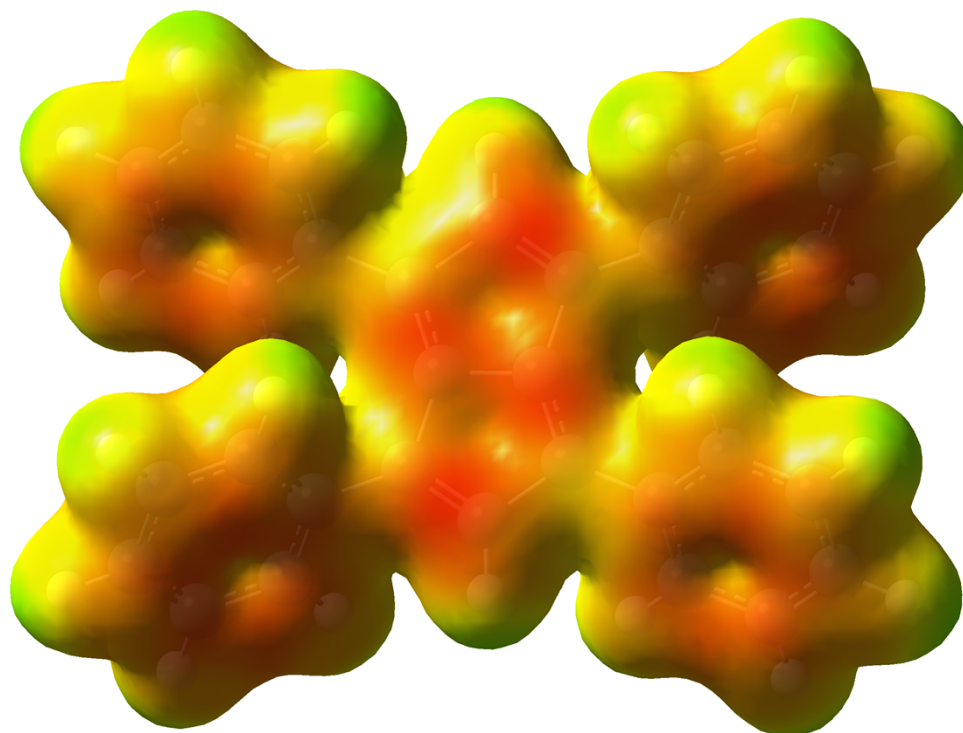
Figure S10: Electrostatic potential (ESP) map for **Ph₄Pn**. Contour colours range from −0.036 (red) to 0.3 (blue) at an isovalue of 0.01.
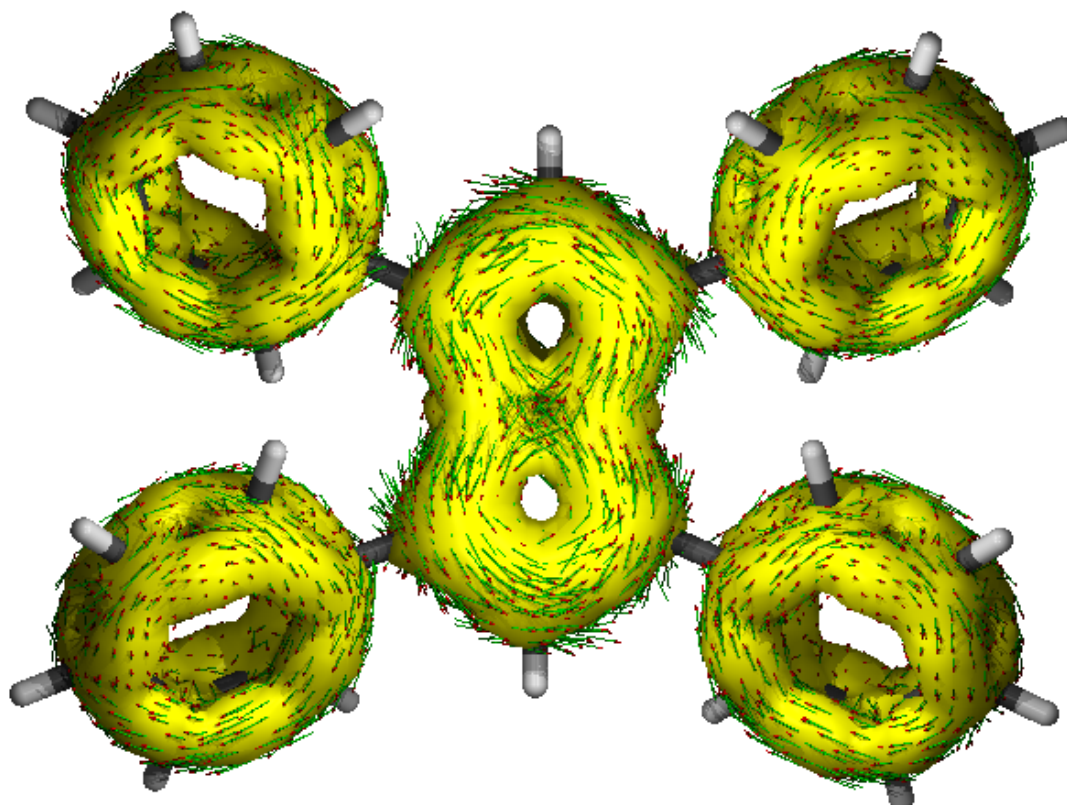
Figure S11: ACID plot of **Ph₄Pn** visualized with an isovalue of 0.03. Calculated using DFT calculations at the B3LYP/6-311++g(d,p) level of theory.
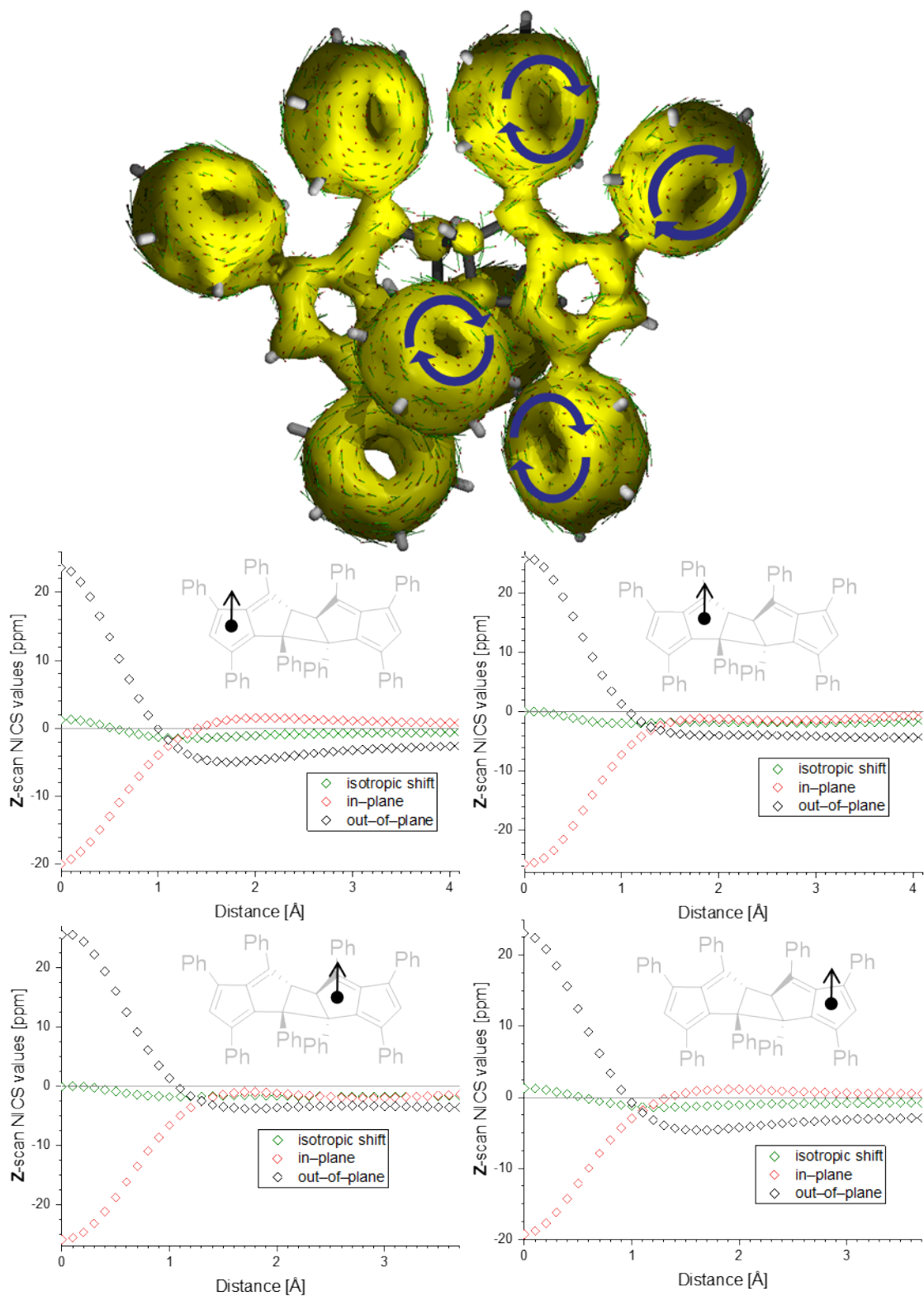
Figure S12: ACID plot (top; iso-value = 0.015) and NICS Z scans of the respective five-membered cycle in **[Ph₄Pn]₂** indicated by the positioning of the arrow in the structure; NICS probe BQ shown as • of the cycloaddition product. All calculated using DFT calculations at the B3LYP/6-311++g(d,p) level of theory.
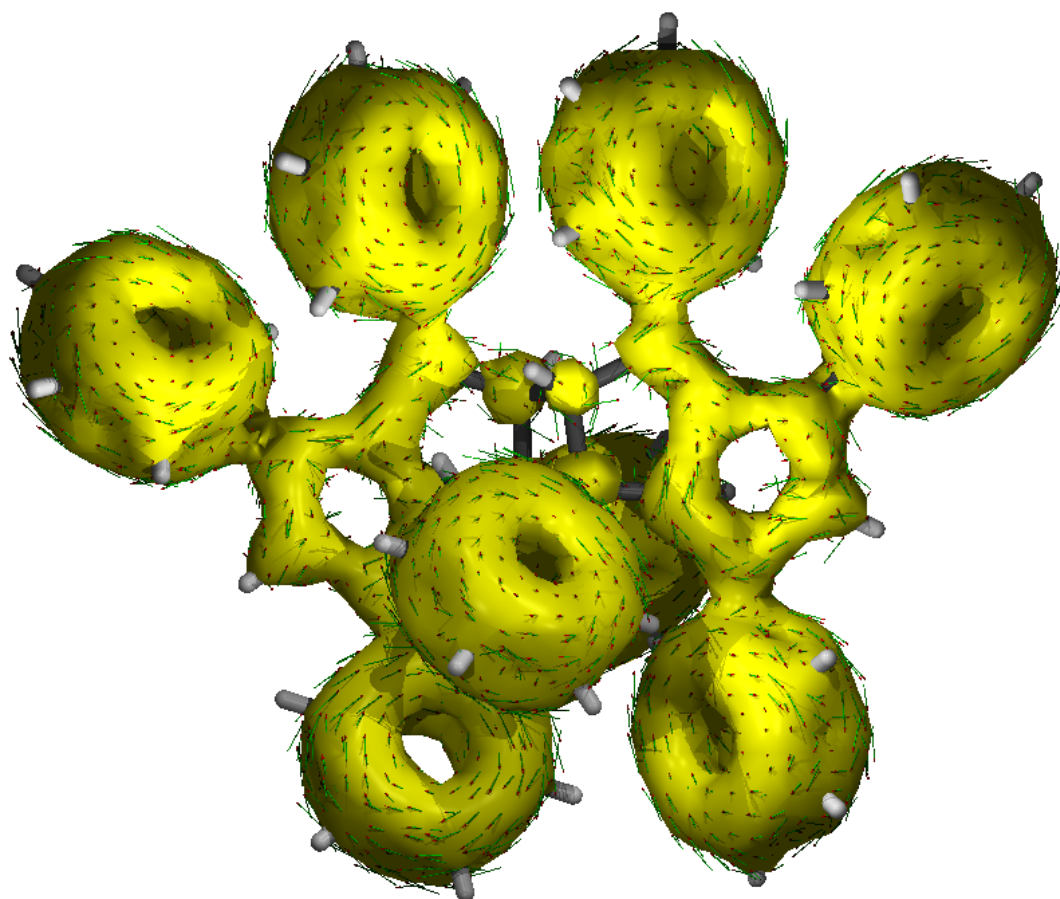
Figure S13: ACID plot of the cycloaddition product **[Ph₄Pn]₂** visualized with an isovalue of 0.015. Calculated using DFT calculations at the B3LYP/6-311++g(d,p) level of theory.
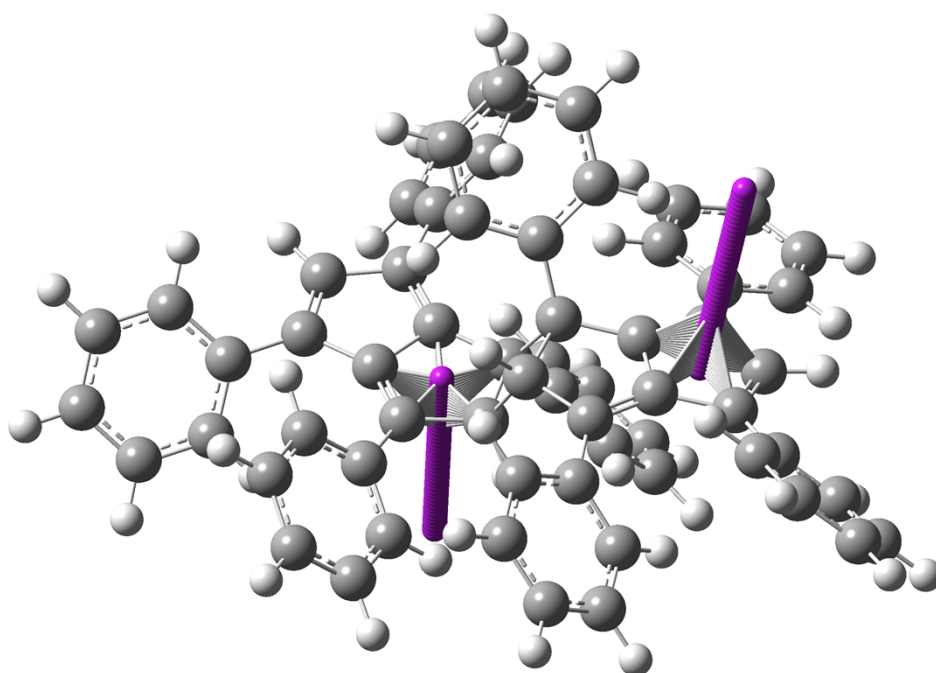
Figure S14: Placement of the Bq atoms for the NICS Z scan of two five-membered rings in **[Ph₄Pn]₂**.
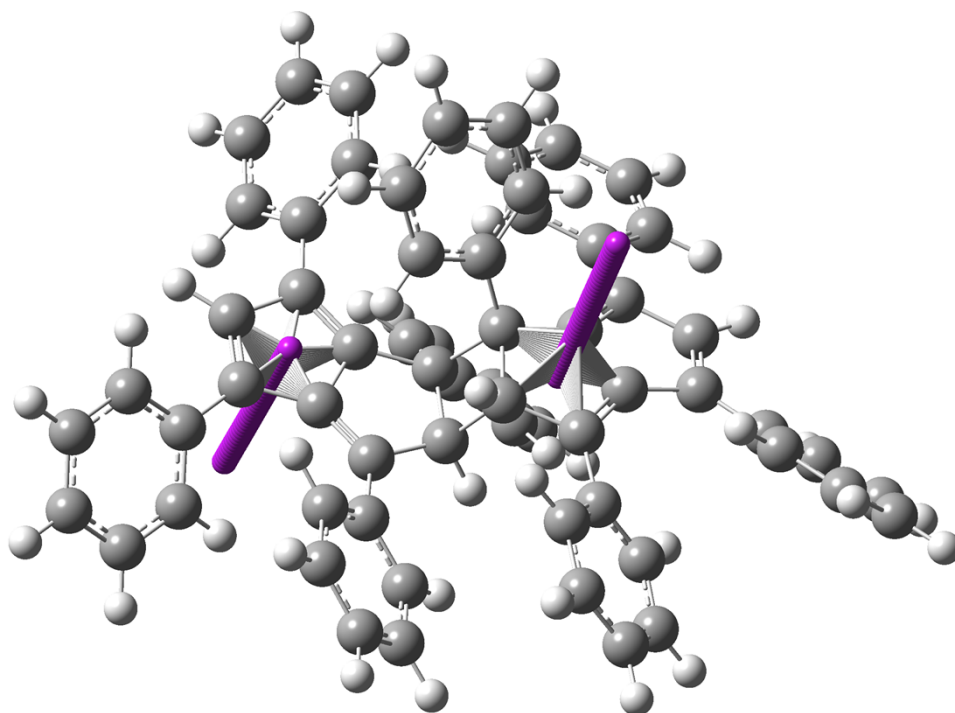
Figure S15: Placement of the Bq atoms for the NICS Z scan of the other two five-membered rings in [Ph$_4$Pn]$_2$.
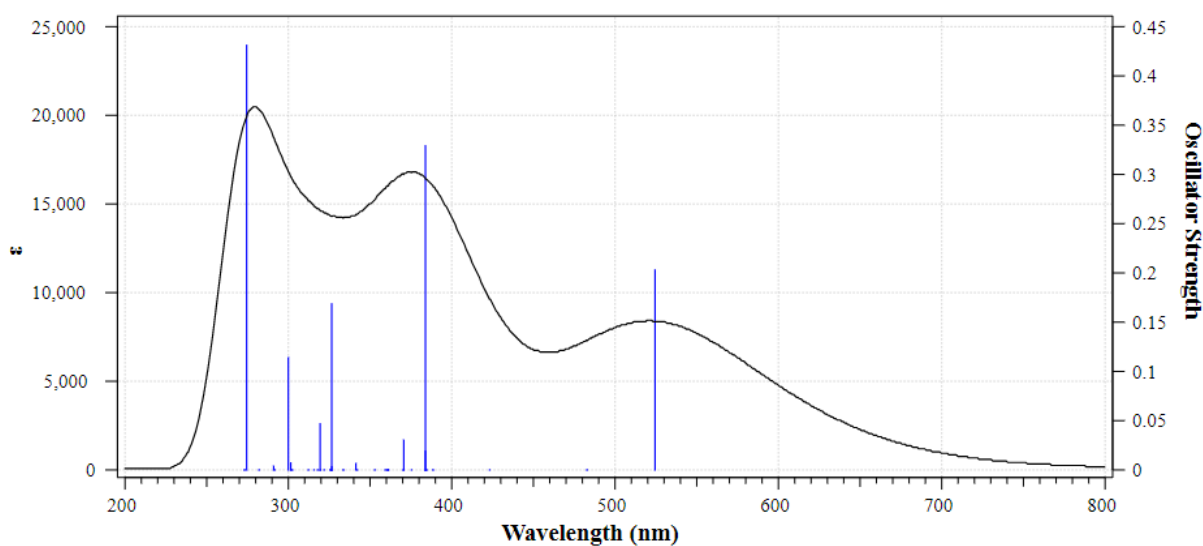
Figure S16: TD-DFT of singlet **Ph₄Pn** performed at the B3LYP/6-311++g(d,p) level of theory in the gas phase. Graphic was obtained via the standard Gaussian plot function.
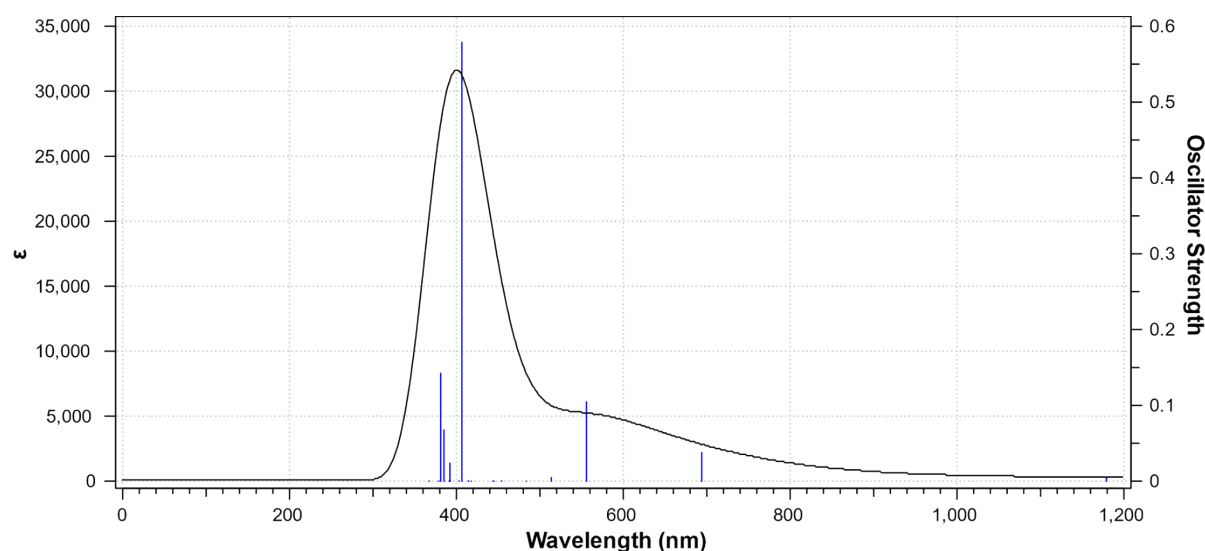
Figure S17: TD-DFT of triplet **Ph₄Pn** performed at the B3LYP/6-311++g(d,p) level of theory in the gas phase. Graphic was obtained via the standard Gaussian plot function.

Electrochemistry

Cyclic voltammetry was performed inside a MBraun Unilab Plus Glovebox using a three-electrode cell and an Ivium Technologies CompactStat. 0.1 M [NBu$_4$][PF$_6$] electrolyte in THF, a graphitic carbon working electrode, platinum wire counter electrode and a Ag/Ag$^+$ pseudo reference electrode (0.01 M AgPF$_6$ in THF) were used at ambient temperature. Potentials were referenced to the normal hydrogen electrode (NHE) by means of the following equation:[15]

$$E_{(NHE)} = E_{(Ag/AgNO_3)} + 0.197$$

$E_{Red1} = Ph_4Pn + 2e^- \rightarrow Ph_4Pn^{2-}$

$E_{Ox1} = Ph_4Pn^{2-} \rightarrow Ph_4Pn^{\cdot-} + e^-$

$E_{Ox2} = Ph_4Pn^{\cdot-} \rightarrow Ph_4Pn + e^-$
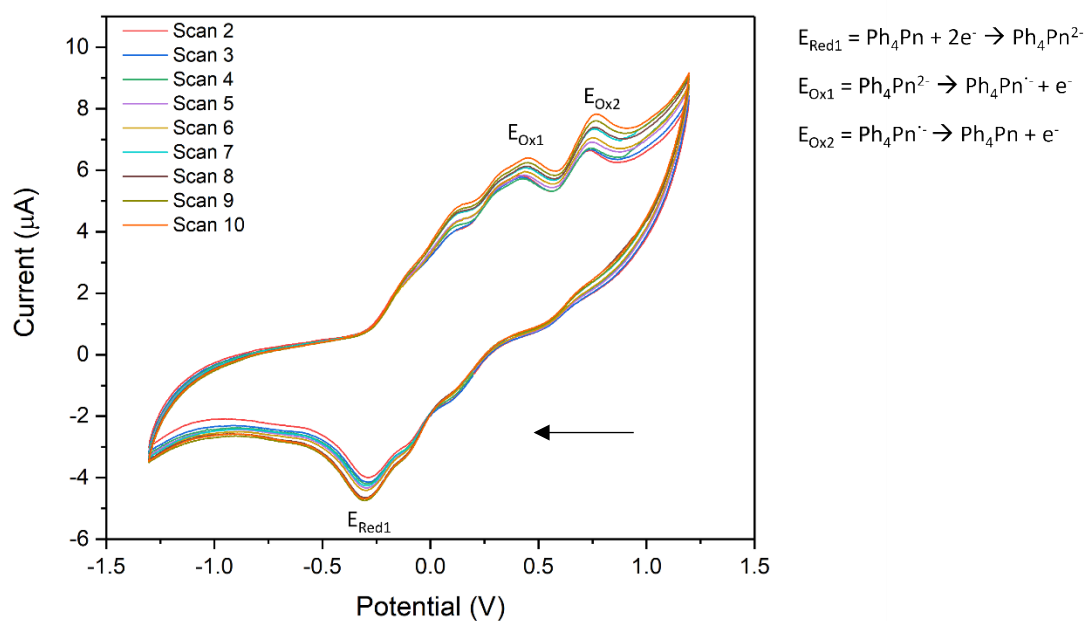
Figure S18: CV of **Ph$_4$Pn** in THF at 1.6 mM recorded at a scan rate of 25 mVs^{-1} with a step size of 5 mV.
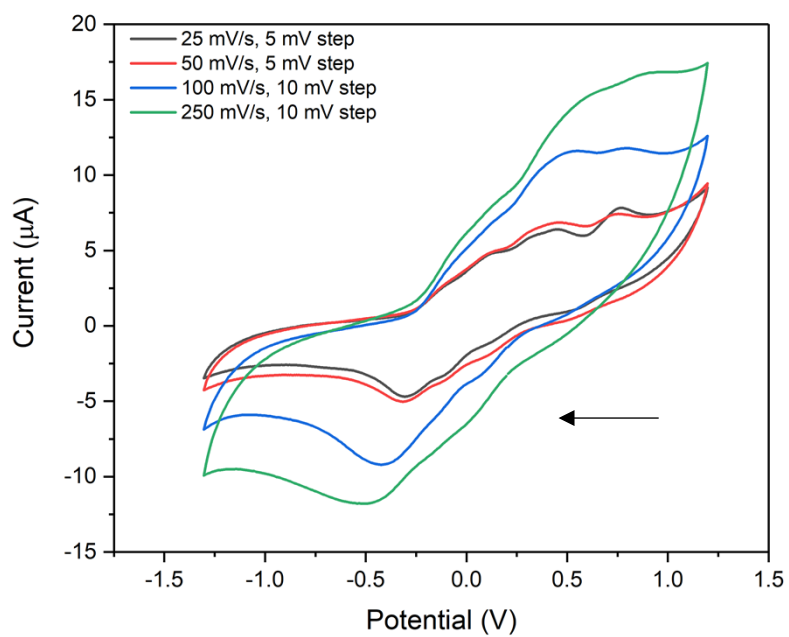
Figure S19: CV of **Ph$_4$Pn** recorded at varying scan rates.
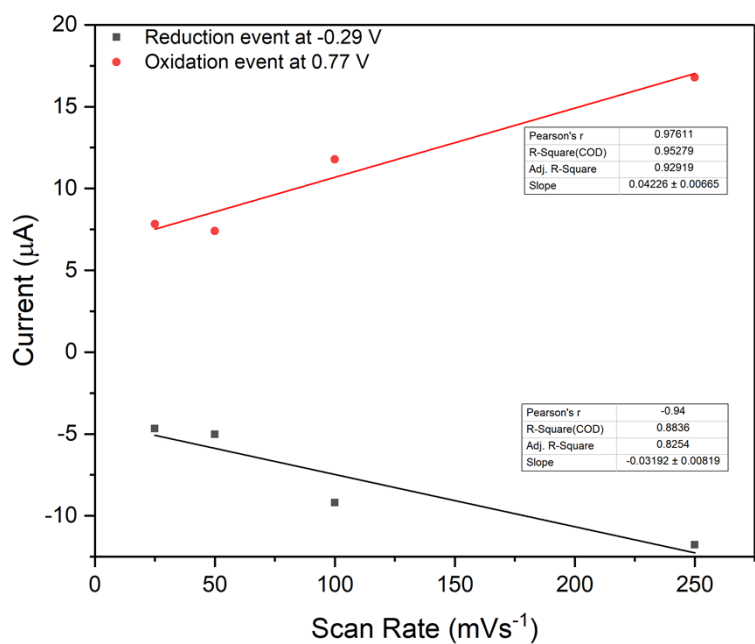
Figure S20: Randles-Sevcik plot of **Ph$_4$Pn**.

Crystallographic Data

CCDC	**2335451**
Identification code	s21uh10
Empirical formula	$C_{166} H_{123}$
Formula weight	2117.64
Temperature	150.00(10) K
Wavelength	1.54184 Å
Crystal system	monoclinic
Space group	C2/c
Unit cell dimensions	a = 43.6143(9) Å α = 90°
	b = 10.5720(2) Å β = 98.309(2)°
	c = 25.1335(7) Å γ = 90°
Volume	11467.2(5) Å^3
Z	4
Density (calculated)	1.227 Mg/m^3
Absorption coefficient	0.523 mm^{-1}
F(000)	4476
Crystal size	0.279 x 0.110 x 0.020 mm^3
Theta range for data collection	4.306 to 73.064°
Index ranges	-53<=h<=51, -8<=k<=13, -30<=l<=31
Reflections collected	49934
Independent reflections	11373 [R(int) = 0.0570]
Completeness to theta = 67.684°	100.0 %
Absorption correction	Semi-empirical from equivalents
Max. and min. transmission	1.00000 and 0.89168
Refinement method	Full-matrix least-squares on F^2
Data / restraints / parameters	11373 / 36 / 778
Goodness-of-fit on F^2	1.012
Final R indices [I>2sigma(I)]	R1 = 0.0449, wR2 = 0.0994
R indices (all data)	R1 = 0.0655, wR2 = 0.1093
Extinction coefficient	n/a
Largest diff. peak and hole	0.216 and -0.223 e.Å^{-3}

References

(1)   Boyt, S. M.; Jenek, N. A.; Sanderson, H. J.; Kociok-Köhn, G.; Hintermair, U. Synthesis of a Tetraphenyl-Substituted Dihydropentalene and Its Alkali Metal Hydropentalenide and Pentalenide Complexes. *Organometallics* **2022**, *41* (3), 211–225. https://doi.org/10.1021/acs.organomet.1c00495.

(2)   Sanderson, H. J.; Kociok-Köhn, G.; Hintermair, U. Synthesis, Structure, and Reactivity of Magnesium Pentalenides. *Inorg. Chem.* **2023**, *62* (39), 15983–15991. https://doi.org/10.1021/ACS.INORGCHEM.3C02087.

(3)   Stanger, A. Nucleus-Independent Chemical Shifts (NICS): Distance Dependence and Revised Criteria for Aromaticity and Antiaromaticity. *J. Org. Chem.* **2006**, *71* (3), 883–893. https://doi.org/10.1021/JO051746.

(4)   Gershoni-Poranne, R.; Stanger, A. The NICS-XY-Scan: Identification of Local and Global Ring Currents in Multi-Ring Systems. *Chem. - A Eur. J.* **2014**, *20* (19), 5673–5688. https://doi.org/10.1002/CHEM.201304307.

(5)   Herges, R.; Geuenich, D. Delocalization of Electrons in Molecules. *J. Phys. Chem. A* **2001**, *105* (13), 3214–3220. https://doi.org/10.1021/JP0034426.

(6)   Geuenich, D.; Hess, K.; Köhler, F.; Herges, R. Anisotropy of the Induced Current Density (ACID), a General Method to Quantify and Visualize Electronic Delocalization. *Chem. Rev.* **2005**, *105* (10), 3758–3772. https://doi.org/10.1021/CR0300901.

(7)   Frisch, M. J.; Trucks, G. W.; Schlegel, H. B.; Scuseria, G. E.; Robb, M. A.; Cheeseman, J. R. Scalmani, G.; Barone, V.; Petersson, G. A.; Nakatsuji, H.; Li, X.; Caricato, M.; Marenich, A. V.; Bloino, J.; Janesko, B. G.; Gomperts, R.; Mennucci, B.; Hratchian, H. P.; Ortiz, J. V.; Izmaylov, A. F.; Sonnenberg, J. L.; Williams-Young, D.; Ding, F.; Lipparini, F.; Egidi, F.; Goings, J.; Peng, B.; Petrone, A.; Henderson, T.; Ranasinghe, D.; Zakrzewski, V. G.; Gao, J.; Rega, N.; Zheng, G.; Liang, W.; Hada, M.; Ehara, M.; Toyota, K.; Fukuda, R.; Hasegawa, J.; Ishida, M.; Nakajima, T.; Honda, Y.; Kitao, O.; Nakai, H.; Vreven, T.; Throssell, K.; Montgomery, J. A., J.; Peralta, J. E.; Ogliaro, F.; Bearpark, M. J.; Heyd, J. J.; Brothers, E. N.; Kudin, K. N.; Staroverov, V. N.; Keith, T. A.; Kobayashi, R.; Normand, J.; Raghavachari, K.; Rendell, A. P.; Burant, J. C.; Iyengar, S. S.; Tomasi, J.; Cossi, M.; Millam, J. M.; Klene, M.; Adamo, C.; Cammi, R.; Ochterski, J. W.; Martin, R. L.; Morokuma, K.; Farkas, O.; Foresman, J. B.; Fox, D. J. Gaussian 16, Revision C.01. Gaussian Inc.: Wallingford CT 2016.

(8)   Dirac, P. A. M. Quantum Mechanics of Many-Electron Systems. *Proc. R. Soc. London. Ser. A, Contain. Pap. a Math. Phys. Character* **1929**, *123* (792), 714–733. https://doi.org/10.1098/RSPA.1929.0094.

(9)   Slater, J. C. A Simplification of the Hartree-Fock Method. *Phys. Rev.* **1951**, *81* (3), 385. https://doi.org/10.1103/PhysRev.81.385.

(10)   Becke, A. D. Density-Functional Exchange-Energy Approximation with Correct Asymptotic Behavior. *Phys. Rev. A* **1988**, *38* (6), 3098. https://doi.org/10.1103/PhysRevA.38.3098.

(11)   Lee, C.; Yang, W.; Parr, R. G. Development of the Colle-Salvetti Correlation-Energy Formula into a Functional of the Electron Density. *Phys. Rev. B* **1988**, *37* (2), 785. https://doi.org/10.1103/PhysRevB.37.785.

(12)   Becke, A. D. Density-functional Thermochemistry. III. The Role of Exact Exchange. *J. Chem. Phys.* **1993**, *98* (7), 5648–5652. https://doi.org/10.1063/1.464913.

(13)   Deglmann, P.; Furche, F.; Ahlrichs, R. An Efficient Implementation of Second Analytical Derivatives for Density Functional Methods. *Chem. Phys. Lett.* **2002**, *362* (5–6), 511–518. https://doi.org/10.1016/S0009-2614(02)01084-9.

(14)   Deglmann, P.; Furche, F. Efficient Characterization of Stationary Points on Potential Energy Surfaces. *J. Chem. Phys.* **2002**, *117* (21), 9535–9538. https://doi.org/10.1063/1.1523393.

(15)   Kratochvil, B.; Lorah, E.; Garber, C. Silver-Silver Nitrate Couple as Reference Electrode in Acetonitrile. *Anal. Chem.* **1969**, *41* (13), 1793–1796. https://doi.org/10.1021/AC60282A011.